Environmental Pollution 366 (2025) 125483

Contents lists available at ScienceDirect

Environmental Pollution

journal homepage: www.elsevier.com/locate/envpol

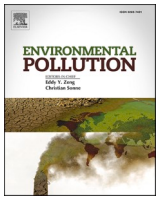

Existence of hydroxymethanesulfonate (HMS) during spring haze and sandstorm events in Beijing: Implications for a heterogeneous formation pathway on mineral aerosols

Yunzhi Xu [a], Tao Ma [b,**], Fengkui Duan [a,*], Shuxiao Wang [a], Jingkun Jiang [a], Yafang Cheng [c], Hang Su [d], Taicheng An [b], Yongliang Ma [a], Takashi Kimoto [e], Tao Huang [e], Kebin He [a]

[a] State Key Joint Laboratory of Environment Simulation and Pollution Control, School of Environment, State Environmental Protection Key Laboratory of Sources and Control of Air Pollution Complex, Beijing Key Laboratory of Indoor Air Quality Evaluation and Control, Tsinghua University, Beijing, 100084, China
[b] Guangdong-Hong Kong-Macao Joint Laboratory for Contaminants Exposure and Health, Guangdong Key Laboratory of Environmental Catalysis and Health Risk Control, School of Environmental Science and Engineering, Institute of Environmental Health and Pollution Control, Guangdong University of Technology, Guangzhou, 510006, China
[c] Aerosol Chemistry Department, Max Planck Institute for Chemistry, Mainz, 55128, Germany
[d] State Key Laboratory of Atmospheric Environment and Extreme Meteorology, Institute of Atmospheric Physics, Chinese Academy of Sciences, Beijing, 100029, China
[e] Kimoto Electric Co., Ltd., 3-1 Funahashi-Cho, Tennouji-Ku, Osaka, 543-0024, Japan

ARTICLE INFO

Keywords:
Hydroxymethanesulfonate
Haze
Sandstorm
Aerosol water content
pH
Mineral aerosol

ABSTRACT

Hydroxymethylsulfonate (HMS) is an abundant secondary organic aerosol from aqueous or heterogeneous processes and may be misidentified as sulfate in conventional measurements. High concentrations of HMS have been observed in humid winter and autumn haze in northern China, while its prevalence in other seasons is unclear and the production medium is controversial. In this study, our field measurements in Beijing during the 2021 spring first showed the presence of HMS in $PM_{2.5}$ during both haze and sandstorm events despite the different atmospheric conditions. HMS accounted for 0.44% of $PM_{2.5}$ during haze periods, higher than the proportion (0.097%) during sandstorms. The sum of HMS and sulfate was also higher during the haze (6.5 μg m^{-3}) than during the sandstorm (2.6 μg m^{-3}), while the HMS/sulfate molar ratio during the haze (0.021) was similar to the value during the sandstorm (0.019). HMS concentration showed a good positive correlation with aerosol water content (AWC), indicating multiphase production. During haze periods, relatively high AWC favored the formation of HMS. In contrast, relative humidity and AWC decreased significantly during sandstorm events, while high pH favored HMS formation. In addition, higher concentrations and proportions of HMS were observed in $PM_{2.5-10}$ than in $PM_{2.5}$. The presence of HMS in dust particles indicated a heterogeneous formation mechanism of HMS on mineral aerosols. Our findings broaden the prevalence of HMS in aerosols and indicate a new HMS formation mechanism from the perspective of observation.

1. Introduction

Particulate matter (PM) pollution is a worldwide environmental problem, especially in the North China Plain (An et al., 2019; Chu et al., 2020; Zhao et al., 2024), with adverse effects on air quality, human health, and climate (Geng et al., 2021; Li et al., 2022; Shaddick et al., 2020). PM comes from both natural and anthropogenic sources, and pollution in urban areas is mainly influenced by anthropogenic sources (Zhang et al., 2015). Unlike the London smog and the Los Angeles photochemical smog, China's haze pollution is more complex with the co-existing strong homogenous nucleation and multi-phase/heterogeneous processes (Chu et al., 2020). With the implementation of a series of clean air policies in recent years by the Chinese government, anthropogenic emissions have dropped significantly and air quality has improved (Zhang et al., 2019; Zheng et al., 2018). However, the frequency of extreme weather events, such as sandstorms (Wang et al., 2022), increased in recent years (Li et al., 2021a), exacerbating pollution and leading to additional adverse health effects

* Corresponding author.
** Corresponding author.
E-mail addresses: matao@gdut.edu.cn (T. Ma), duanfk@tsinghua.edu.cn (F. Duan).

https://doi.org/10.1016/j.envpol.2024.125483
Received 8 June 2024; Received in revised form 2 December 2024; Accepted 4 December 2024
Available online 5 December 2024

(Zhang et al., 2020).

Strong sandstorms resurged in 2021 after an absence of more than ten years (Yin et al., 2022). During these sandstorm episodes, the hourly peak concentration of PM_{10} (particulate matter with an aerodynamic diameter ≤10 μm) in Beijing reached 5267.7 μg m^{-3} (Liu et al., 2023). The resurgence of severe sandstorms has made China's air pollution situation even more complex, especially when sandstorms coincide with haze pollution (Liu et al., 2023). A great contribution of anthropogenic emissions has an impact on the areas downwind of the sandstorm in China (Yu et al., 2023). Cheng et al. (2022) observed $PM_{2.5}$ (particulate matter with an aerodynamic diameter ≤2.5 μm) in the spring of 2021 and identified emission sources by the positive matrix factorization (PMF) model in Lanzhou, a city in northwest China, and found that dust (32.0%) and industrial entities (29.8%) were the top two sources contributing to $PM_{2.5}$ concentration. Zuo et al. (2022) investigated the stable Fe isotopic compositions of magnetic particulate matter during the 2021 Beijing sandstorm episodes, revealing the complexity of $PM_{2.5}$ affected by human sources. The coupling of natural and anthropogenic sources will also enhance the heterogeneous reactions under certain meteorological conditions. Insoluble mineral aerosols can adsorb water (Schuttlefield et al., 2007) and provide a medium for reactions with anthropogenic pollutants like sulfur dioxide (SO_2), nitrogen oxides (NO_x), ammonia (NH_3), and volatile organic compounds (VOCs) (Fu et al., 2016; Kok et al., 2023).

Hydroxymethanesulfonate (HMS, $CH_2(OH)SO_3^-$) is an important organosulfur compound formed by dissolved SO_2 and formaldehyde (HCHO) in aqueous solution and has been reported in cloud water, fog water, and aerosols around the world (Dixon and Aasen, 1999; Eatough and Hansen, 1984; Gilardoni et al., 2016; Munger et al., 1986; Munger et al., 1990; Olson and Hoffmann, 1989; Scheinhardt et al., 2014; Suzuki et al., 2001; Whiteaker and Prather, 2003; Winkelman et al., 2002). Recently, HMS has become a research hotspot again because of its significant contribution to autumn and winter haze pollution in the North China Plain, where HMS concentrations in $PM_{2.5}$ can be up to 18.5 μg m^{-3}, and HMS can be misidentified as sulfate in conventional ion chromatography (IC) and aerosol mass spectrometer (AMS) measurements and lead to an overestimation of sulfate (Chen et al., 2022; Ma et al., 2020; Moch et al., 2018; Song et al., 2019; Wei et al., 2020). It can be used as a tracer of atmospheric secondary reactions in liquid or heterogeneous phases (Dixon and Aasen, 1999; Whiteaker and Prather, 2003). Previous studies proposed that the production medium of HMS in aerosols could be cloud water (Moch et al., 2018), fog water (Liu et al., 2021; Wei et al., 2020), or aerosol water (Ma et al., 2020). So far, reports on HMS in aerosols focused on humid and cold environments like northern China (Chen et al., 2022; Ma et al., 2020; Moch et al., 2018; Song et al., 2019; Wei et al., 2020) and near the Arctic areas (Campbell et al., 2022; Liu et al., 2021), and the prevalence of HMS in the atmosphere is unclear and the medium of production is controversial.

In this study, we first reported the existence of HMS in $PM_{2.5}$ during both haze and sandstorm pollution in Beijing during the 2021 spring. We revealed the different characteristics and influencing factors of HMS formation during haze and sandstorm events in spring. In addition, the distribution of HMS in coarse and fine PM during the sandstorm episodes was investigated. Based on the observation results, we proposed a new HMS formation mechanism on mineral aerosols.

2. Methods

2.1. Field measurements

Online observation and offline sample collection were simultaneously conducted on the rooftop of the School of Economics and Management on the campus of Tsinghua University (40.00° N, 116.34° E) from 14th March to 1st May, 2021.

Hourly average online observations included $PM_{2.5}$ and PM_{10} mass concentrations measured by PM-712 (Kimoto Electric Co., Ltd., Japan), organic carbon (OC) concentrations in $PM_{2.5}$ measured by APC-710 (Kimoto Electric Co., Ltd., Japan), SO_2 concentrations measured by SA-731 (Kimoto Electric Co., Ltd., Japan), and O_3 concentrations measured by OA-781 (Kimoto Electric Co., Ltd., Japan). The hourly meteorological parameters were measured with an automatic meteorological observation instrument (Milos 520, VAISALA Inc., Finland). A detailed description of the instruments can be found in our previous studies (Duan et al., 2006; Li et al., 2018; Li et al., 2021b; Xu et al., 2017; Yang et al., 2018). A factor of 1.6 was used to convert the OC mass into organic matter (OM) mass (Xing et al., 2013).

Day and nighttime samples of $PM_{2.5}$ were collected on 90-mm-diameter quartz filters at a flow of 100 L min^{-1} by Laoying-2030 sampler (Qingdao Laoying Haina Opto-electronic Environmental Protection Group Co., Ltd., China) from 7th April to 1st May, 2021. The above samples were used for analyzing different characteristics and influencing factors of HMS formation in Sections 3.1 and 3.2. Furthermore, nine daily samples of $PM_{2.5}$ and $PM_{2.5-10}$ (particulate matter with an aerodynamic diameter from 2.5 to 10 μm) during sandstorm periods in March and April 2021 were collected by AS250D sampler (Kimoto Electric Co., Ltd., Japan) using 47-mm-diameter quartz filters at a flow rate of 15.4 L min^{-1} and 20-mm-diameter quartz filters at a flow rate of 1.3 L min^{-1}, respectively. These samples were used for the size distribution analysis of HMS in Section 3.3. All the filters were baked at 550 °C for 6 h before sampling. After sampling, the filters were put in the cassettes, packed using aluminum foil to avoid light, and then stored at −20 °C before analysis.

2.2. HMS quantitation by ion chromatography

The detailed analytical method of HMS has been described in our previous study (Ma et al., 2020). Samples of 90-mm-diameter quartz filters were cut by a 2-cm-diameter circular punch, 47-mm-diameter filters were cut into four quarters and one part was taken, and 20-mm-diameter filters were fully used. Then the filters were extracted twice with 5 mL 0.1% HCHO solution, treated with ultrasonic agitation in an ice bath for 20 min each time, and then filtered through the 0.45 μm membrane syringe filters. Two extracts were synthesized for subsequent analysis. A dilute solution of 0.1% HCHO was designed to counteract the HMS decomposition during the pretreatment process since HMS would gradually convert to sulfate over time in samples extracted by water (Ma et al., 2020).

The solutions were then injected into a Dionex Integration HPIC ion chromatography system with an AS11-HC analytical column and AG11-HC guard column (Dionex Corp., CA, USA) for the anion analysis. We used an eluent of 11 mM KOH with a flow rate of 1.5 mL min^{-1} for the complete separation of HMS and sulfate peak. Fig. S1(a) and (c) show the peak of HMS and sulfate in standard solutions, and Fig. S1(b) and (d) show the standard curves with $R^2 = 0.999$. Fig. S1(e) shows the chromatogram of the solution extracted from a $PM_{2.5}$ sample in this study. The detection limit is 0.02 mg L^{-1}, and values below the detection limit are treated as 0.

F_{HMS} and $F_{sulfate}$ were used to calculate the fraction of HMS and sulfate in total sulfur by equations (1) and (2), respectively:

$$F_{HMS} = \frac{n[HMS]}{n[HMS] + n[SO_4^{2-}] + n[SO_2]} \quad (1)$$

$$F_{sulfate} = \frac{n[SO_4^{2-}]}{n[HMS] + n[SO_4^{2-}] + n[SO_2]} \quad (2)$$

where n refers to the molar concentration.

2.3. ISORROPIA-II thermodynamic equilibrium model calculation

Aerosol water content (AWC) and pH were calculated using the ISORROPIA-II thermodynamic equilibrium model. The forward model is

constrained by the measurements of gases (HNO_3, HCl, and NH_3) and aerosols (SO_4^{2-}, NO_3^-, Cl^-, K^+, Ca^{2+}, Na^+, Mg^{2+}, and NH_4^+), and the aerosol phase state is assumed to be metastable (Fountoukis and Nenes, 2007; Nenes et al., 2020). Input data were attained by the online gases and aerosols monitoring instrument MARGA (Metrohm Ltd., Switzerland) at an hourly resolution (Fig. S2). More details and principles of MARGA can be found in previous studies (Chen et al., 2017; Rumsey et al., 2014). MARGA was set on the roof of the Suez Environmental Science and Engineering Experimental Practice Teaching Center in the northwest area of Tsinghua University, which was less than 1 km away from the School of Economics and Management. Considering that aerosols are unlikely to be completely liquid at low relative humidity (RH), data with RH<20% were excluded when calculating pH (Guo et al., 2016). Fig. S3 and Fig. S4 show the comparisons between the simulated and measured NH_3(g), NH_4^+(p), HNO_3(g), and NO_3^-(p) during haze and sandstorm, respectively. The predicted and measured NH_3(g), NH_4^+(p) and NO_3^-(p) values were in good agreement with about 0.9 *r* values and approximately 1 slope values. However, the measured and predicted partitioning of HNO_3(g) during haze and sandstorm showed significant discrepancies (*r* values of 0.43 and 0.57, respectively), which may be attributed to the much lower gas concentrations than particle concentrations, as well as the HNO_3 measurement uncertainties from MARGA (Ding et al., 2019; Rumsey et al., 2014).

3. Results and discussion

3.1. General characteristics of HMS in spring haze and sandstorms

In this study, we observed three HMS pollution episodes (EP-1/2/3) in April, as shown in Fig. 1 (see detailed data in Table S1). HMS pollution episodes were classified based on continuous HMS detection and over two days duration. EP-2 was related to an extremely severe sandstorm event (Liu et al., 2023; Yin et al., 2022; Zuo et al., 2022), which was accompanied by a sharp increase in PM_{10} concentration and a decrease in $PM_{2.5}/PM_{10}$ ratio and RH. The maximum hourly concentration of PM_{10} and $PM_{2.5}$ reached 1065.7 μg m^{-3} and 318.6 μg m^{-3} at 17:00 on April 15th, respectively. EP-1 and EP-3 were related to haze pollution with hourly $PM_{2.5}$ above 35 μg m^{-3} (the Grade I guideline of daily $PM_{2.5}$ concentration in Chinese National Ambient Air Quality Standard GB 3095–2012) and $PM_{2.5}/PM_{10}$ mass ratio over 50%. During the haze pollution processes, $PM_{2.5}$ and PM_{10} concentrations simultaneously increased with high $PM_{2.5}/PM_{10}$ ratios (>60%) under relatively high RH, similar to previous studies (Li et al., 2018; Yang et al., 2018; Zheng et al., 2015). The $PM_{2.5}$ concentration levels during the haze periods (EP-1 and EP-3, 40.7 ± 19.0 μg m^{-3}) were close to that during the sandstorm period (EP-2, 52.2 ± 53.5 μg m^{-3}), but the PM_{10} concentrations were much lower than the value during the sandstorm period (68.4 ± 31.7 μg m^{-3} *vs.* 174.1 ± 208.1 μg m^{-3}).

Our field measurements confirmed the existence of HMS in $PM_{2.5}$ during both haze and sandstorm events in spring (Fig. 1). HMS showed a consistent trend with inorganic sulfate and organic matters (OM) during the two types of pollution (Fig. S5). The average HMS concentration during April was 0.066 ± 0.098 μg m^{-3} with a maximum value of 0.44 μg m^{-3}. The mean concentrations of HMS, sulfate, and OM in $PM_{2.5}$ were 0.16 ± 0.10 μg m^{-3}, 6.4 ± 2.0 μg m^{-3}, and 10.3 ± 5.2 μg m^{-3} during the haze and 0.067 ± 0.10 μg m^{-3}, 2.5 ± 2.0 μg m^{-3}, and 9.7 ± 7.0 μg m^{-3} during the sandstorm, respectively. HMS concentrations in Beijing were lower in spring than in autumn and winter (Chen et al., 2022; Ma et al., 2020; Wei et al., 2020), but still higher compared to other regions of the world (Table S2). The average HMS concentration was 1–2 orders of magnitude higher than that measured in the Arctic (Liu et al., 2021) and was 2–15 times larger than observation values in the US (Dixon and Aasen, 1999) and Japan (Suzuki et al., 2001) during the same season.

The contribution of HMS was more significant during the haze periods compared with the sandstorm. The proportion of HMS to $PM_{2.5}$ mass increased from 0.097% during the sandstorm to 0.44% during the haze. Correspondingly, HMS accounted for 1.9% of OM during the haze periods, which was much higher than that during the sandstorm (0.5%) and was close to the overall level in the 2015 winter by Ma et al. (2020) (Fig. 2(a)).

As shown in Fig. 3(a) and (b), the concentration of HMS and sulfate, two main secondary sulfur species in the particle phase, was higher during the haze than during the sandstorm. F_{HMS} and $F_{sulfate}$ were both higher during the haze periods than during the sandstorm (Fig. 3(c) and (d)), indicating stronger secondary processes. The molar ratio of HMS to sulfate can be used to indicate the distribution of sulfur in the particle phase. The HMS/sulfate molar ratio during the haze (0.021) was similar to the value during the sandstorm (0.019). The molar ratios of HMS to

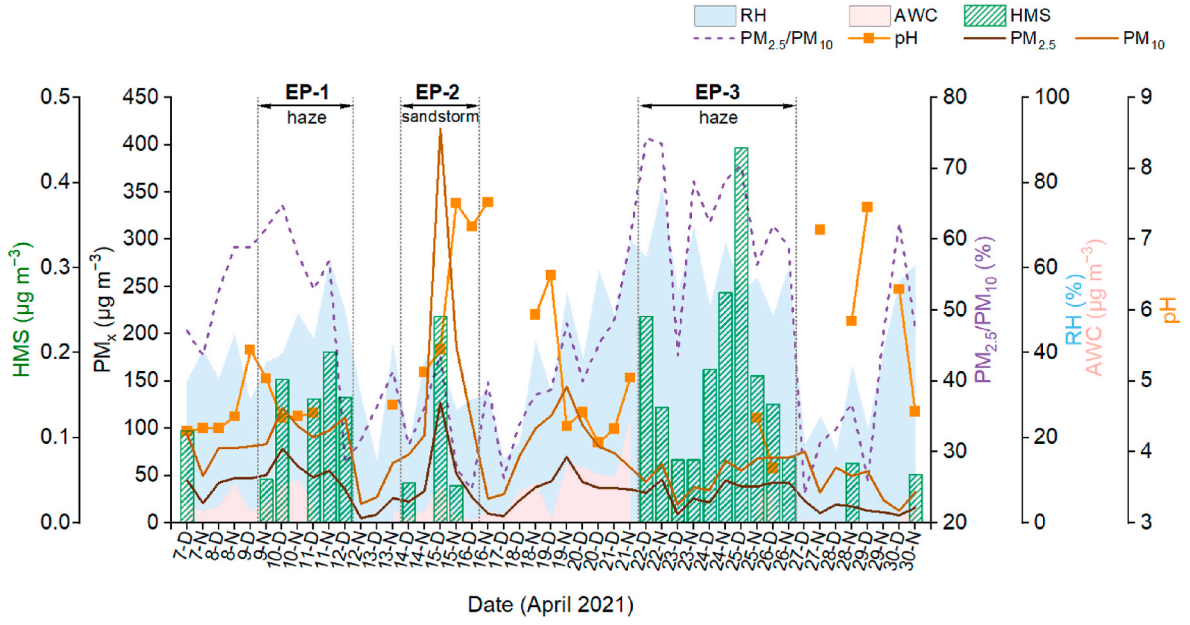

Fig. 1. Characteristics of offline samples in April 2021. Variation of HMS, $PM_{2.5}$, PM_{10}, $PM_{2.5}/PM_{10}$ ratio, relative humidity (RH), aerosol water content (AWC), and aerosol acidity (pH). Numbers in the X-axis label represent the date, D and N refer to Day and Night, respectively. HMS concentrations are derived from offline $PM_{2.5}$ samples measured by the ion chromatography method, while other parameters are averages of online hourly data during sampling periods.

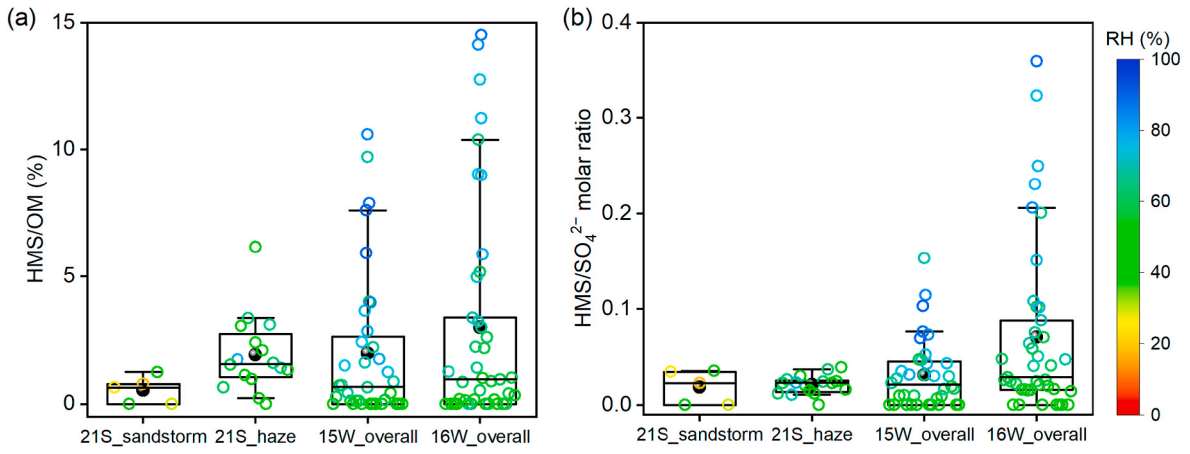

Fig. 2. Box plots of (a) the mass ratio of HMS to OM, and (b) the molar ratio of HMS to sulfate in April 2021 sandstorm and haze (21S_sandstorm and 21S_haze) and previous winter in 2015 (15W_overall) and 2016 (16W_overall) (Ma et al., 2020). The mean (diamond), median (horizontal line), 25th and 75th percentiles (lower and upper box), and 5th and 95th (lower and upper whiskers) are shown. The points are colored by relative humidity (RH).

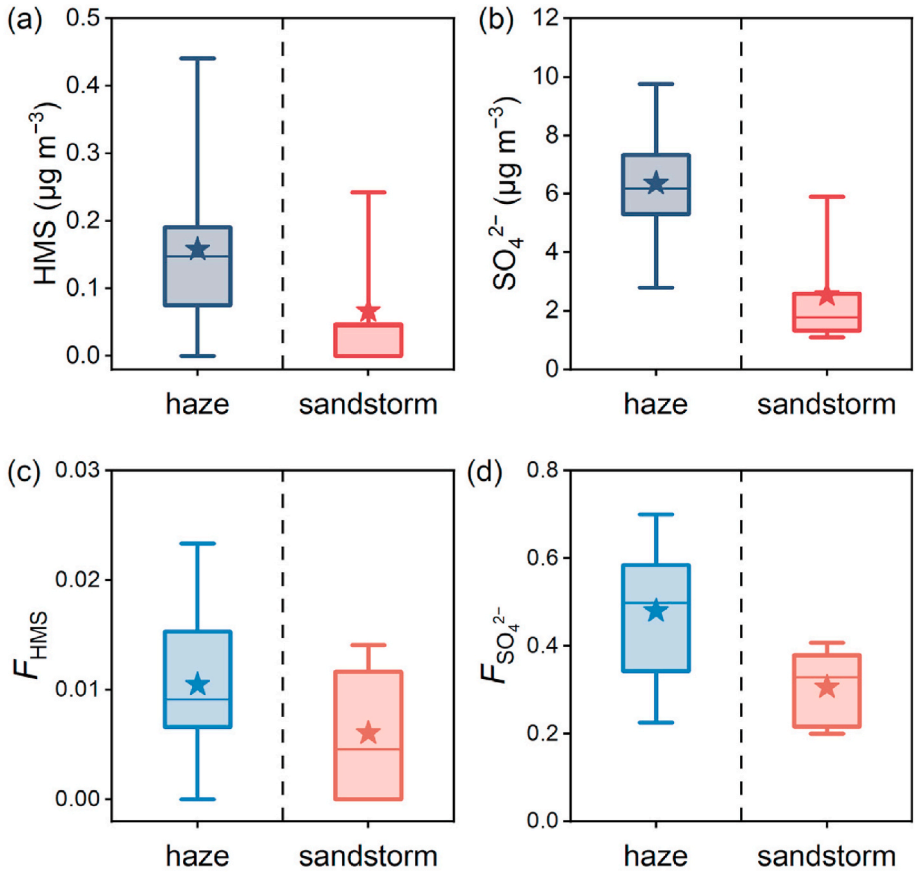

Fig. 3. Comparison of (a) HMS concentration, (b) sulfate concentration, (c) molar fractions of HMS in total sulfur, and (d) molar fractions of sulfate in total sulfur between haze and sandstorm pollution in April 2021. The mean (star), median (horizontal line), 25th and 75th percentiles (lower and upper box), and 5th and 95th percentiles (lower and upper whiskers) are shown.

sulfate during the sandstorm and haze in April 2021 were also comparable to the level of the 2015 winter and lower than the 2016 winter as shown in Fig. 2(b). Therefore, HMS played an important role in PM pollution in both winter and spring. As HMS was a tracer of secondary formation in the atmosphere (Whiteaker and Prather, 2003), the existence of HMS in spring sandstorms suggested that the resurgent sandstorm pollution under current situation had the characteristics of multi-source mixing.

3.2. *Major influencing factors of HMS formation during spring haze and sandstorms*

The favorable factors for HMS formation during haze and sandstorm events were different. As shown in Fig. 4, HMS concentration showed a good positive correlation ($r = 0.89$, $P < 0.001$) with AWC, consistent with winter results (Ma et al., 2020), indicating that aerosol water served as a medium for multiphase HMS production during spring. In

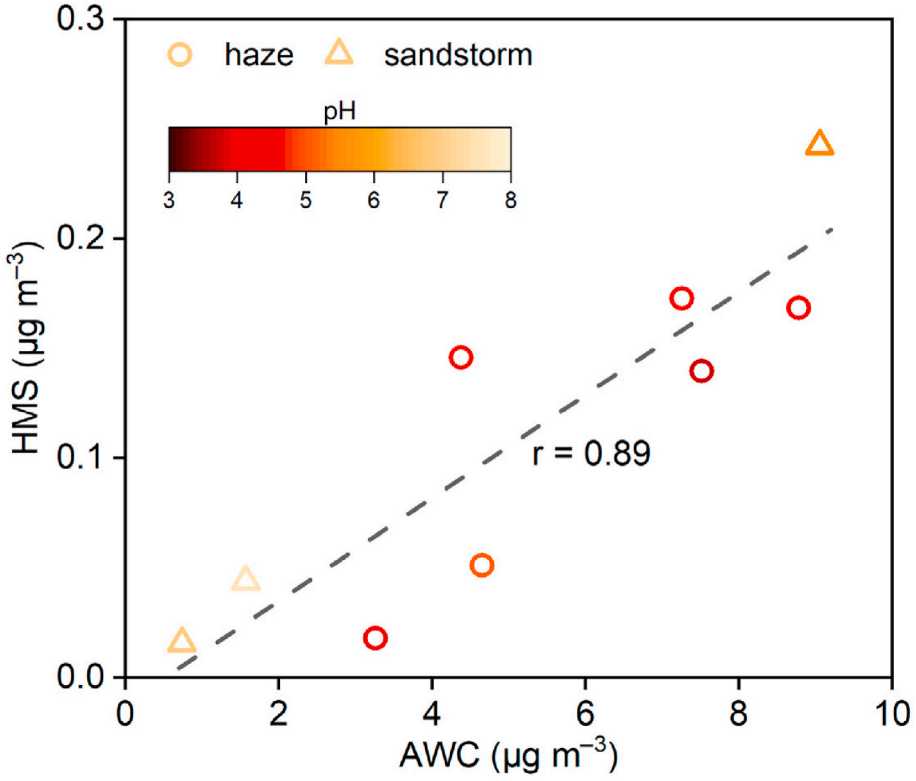

Fig. 4. Correlation between HMS concentration and aerosol water content (AWC) in $PM_{2.5}$. Circles and triangles represent samples during haze and sandstorm episodes, respectively, and are colored by pH. The points are the samples with the information on HMS concentration, AWC, and pH.

addition, HMS concentrations were higher under higher pH conditions under similar AWC levels. Previous studies showed that high concentrations of precursors (SO_2 and HCHO), low oxidant levels, low temperature, high RH and moderately acidic pH favored the HMS formation (Boyce and Hoffmann, 1984; Deister et al., 1986; Ma et al., 2020; Olson and Hoffmann, 1989). Fig. 5 compares the influencing factors of HMS formation during the haze and sandstorm events. The SO_2 concentration, ozone (O_3) concentration, and temperature (T) during the haze and sandstorm periods were similar. Haze episodes presented characteristics of relatively high RH and AWC, providing favorable conditions for multiphase reactions (Bian et al., 2014; Wu et al., 2018). During the haze period (EP-1 and EP-3), the average RH was 55.9% and the AWC increased with RH with an average of 7.5 μg m^{-3} (Fig. S6). The calculations based on the ISORROPIA-II model showed an average aerosol pH value of 4.6 during the haze, consistent with previous results (Ding et al., 2019; Ma et al., 2020). Therefore, the formation of HMS during the spring haze was similar to that during the winter haze, where AWC was a key influencing factor.

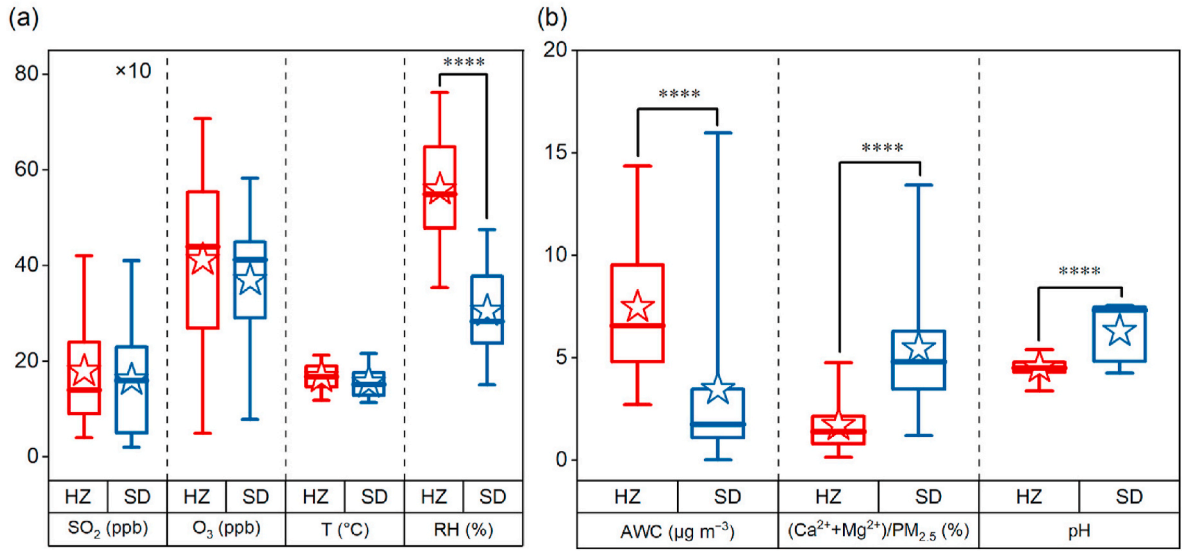

Fig. 5. Comparison of (a) SO_2 concentration, O_3 concentration, temperature (T), relative humidity (RH), and (b) aerosol water content (AWC), the mass percentage of calcium and magnesium ions in $PM_{2.5}$ and pH between haze (HZ) and sandstorm (SD) events in April 2021. In the box-whisker plots, the whiskers, boxes, and pentagrams indicate the 95th, 75th, 50th, 25th, and 5th percentiles and mean values. The **** indicates $P < 0.0001$ of t-test.

During the sandstorm period (EP-2), high pH favored the formation of HMS despite relatively low AWC. The RH was relatively low since high-pressure cyclones from Mongolia (Fig. S7) brought dry air mass, making the average surface RH low to 30.2%. As a result, the average AWC dropped down to 3.1 μg m^{-3} during the sandstorm. Higher aerosol pH has been reported in Inner Mongolia, an arid region in northern China close to the sandstorm source, due to a higher contribution of crustal dust (Wang et al., 2019). A previous study showed that aerosol pH increased from dust contributions (Shi et al., 2017). As shown in Fig. S8, the pH showed a good positive correlation ($r = 0.80$, $P < 0.001$) with the percentage of calcium and magnesium ions in $PM_{2.5}$. Due to the increase of mineral cations such as magnesium and calcium ions, the average pH increased from 4.6 during haze to 6.2 during the sandstorm (Fig. 5(b)). High pH accelerated the formation of HMS since the concentration of HSO_3^- and SO_3^{2-} increased with the increase of pH, which could promote the formation rate of HMS (Munger et al., 1986; Rao and Collett, 1995).

3.3. HMS formation on mineral aerosols

Mineral dust may act as a reactive surface for the heterogeneous formation of HMS during the sandstorm. Laboratory studies and model simulations have shown that acidic gases such as SO_2 appear to undergo fast neutralization reactions with alkaline material in mineral dust (Zhang and Carmichael, 1999). To further explore the formation of HMS in mineral dust, we analyzed daily $PM_{2.5}$ and $PM_{2.5-10}$ samples collected during the sandstorm episodes in the spring of 2021. As shown in Fig. 6, HMS concentration and its contribution to $PM_{2.5-10}$ in the sandstorm samples were higher than those in $PM_{2.5}$. The contribution of HMS to particles increased with particle size, consistent with winter results that HMS contributed more in larger particles (Ma et al., 2020), but different from previous reports in cloud and fog droplets (Reilly et al., 2001; Whiteaker and Prather, 2003). This suggested a possible HMS heterogeneous formation mechanism on the surface of mineral aerosols. A morphology study showed that the dust particles of sandstorms could also incorporated with particles from polluted East Asia to complicate the secondary aerosol formation (Xu et al., 2020). A soluble coating with hydrophilicity was created after the chemical aging of dust (Kok et al., 2023). Previous studies have also identified the adsorption of SO_2 (Huang et al., 2015) and HCHO on mineral dust (Tang et al., 2017; Xu et al., 2011). Therefore, we speculate that HCHO and SO_2 undergo heterogeneous reactions on wet dust surfaces to form HMS.

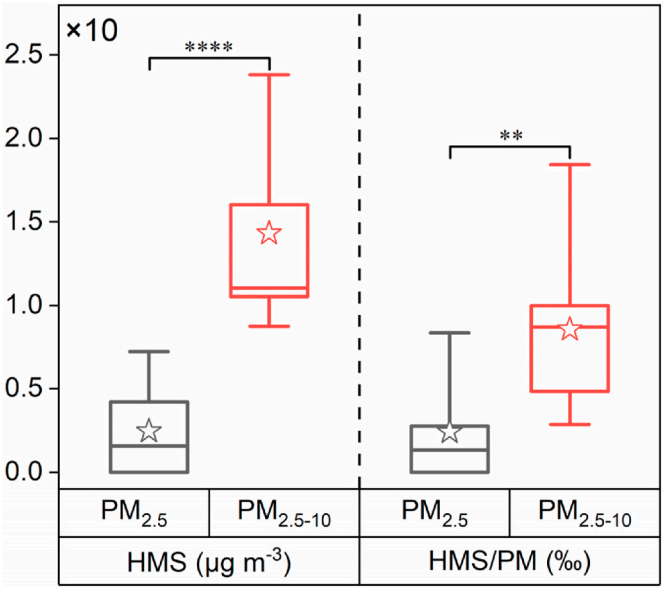

Fig. 6. Comparison of HMS concentration and HMS/PM ratio between $PM_{2.5}$ and $PM_{2.5-10}$ samples during sandstorm events in spring 2021. In the box-whisker plots, the whiskers, boxes, and pentagrams indicate the 95th, 75th, 50th, 25th, and 5th percentiles and mean values. The **** and ** indicate $P <$ 0.0001 and $P < 0.01$ of t-test, respectively.

3.4. Atmospheric implications

Our continuous observations in spring extend the understanding of the seasonal characteristics of HMS and first report the presence of HMS in dust aerosols during sandstorms. The observed HMS concentrations and HMS to sulfate molar ratios in spring were lower than those in northern China during the severe winter haze (Ma et al., 2020; Wei et al., 2020) but higher than those in Europe (Gilardoni et al., 2016; Scheinhardt et al., 2014), America (Campbell et al., 2022; Dixon and Aasen, 1999; Liu et al., 2021; Munger et al., 1986; Whiteaker and Prather, 2003), and Japan (Suzuki et al., 2001). The prevalence of HMS in both fine and coarse particles provides suggestions for air governance that VOCs need to be preferentially controlled despite the significant reduction in SO_2.

Our findings suggest the factors that favor HMS formation in various environments are different. The factors that favor HMS formation in spring haze are similar to those in autumn and winter haze, which depend on the content of aerosol water. An enhancement of HMS formation in aerosol water resulting from the amplified ion strength compared with in bulk water has been investigated by laboratory experiments (Zhang et al., 2023). The latest revision of the GEOS-Chem model has taken into account the contribution of aqueous aerosol chemistry to HMS production (Wang et al., 2024). In contrast, the meteorological conditions in Beijing spring sandstorms have great differences in humidity and pH compared with winter and autumn. The decrease of relative humidity and the consequent decrease of AWC in spring sandstorm episodes seem to be unfavorable for the formation of HMS, but the HMS concentration and its importance in particulate sulfur are still significant under high pH. The heterogeneous formation mechanism of HMS on mineral aerosols is speculated, and more field, laboratory, and modeling work is needed in the future to elucidate the formation mechanism and influencing factors of HMS during sandstorm events.

The presence of HMS in sandstorms indicates that dust particles nowadays are affected by anthropogenic pollution and sandstorms are becoming more complex. Radiative effects from dust aerosols mixed with secondary components may change through interactions with radiation, atmospheric chemistry, clouds, the cryosphere, and biogeochemistry (Kok et al., 2023). In addition, the significant influences of sandstorms by anthropogenic emissions increase their health impacts (Xia et al., 2021). Therefore, more research on the chemical characteristics and processes of sandstorms affected by anthropogenic emissions and their impact on climate and health is needed.

4. Conclusion

In this study, we explored the characteristics and formation mechanism of HMS through field observations in Beijing during the 2021 spring. Despite the different atmospheric conditions, HMS was observed in $PM_{2.5}$ during both haze and sandstorm episodes. The concentrations of HMS increased with the increase of AWC, indicating that aerosol water served as a production medium for HMS. The favorable factors for HMS formation during haze and sandstorms were different. During haze periods, the AWC was relatively high with a moderately acid pH. During the sandstorm periods, higher pH due to a higher content of mineral dust favored the formation of HMS despite relatively low AWC. Furthermore, the size distribution of HMS during sandstorm events showed a higher proportion of HMS in coarse particles. Our field observations indicated the heterogeneous formation of HMS on mineral aerosols. This study broadens the prevalence and formation mechanism of HMS in aerosols and highlights the complexity of recent sandstorms.

CRediT authorship contribution statement

Yunzhi Xu: Writing – original draft, Visualization, Methodology, Investigation, Formal analysis, Data curation. **Tao Ma:** Writing – review & editing, Supervision, Methodology, Funding acquisition, Formal analysis, Data curation, Conceptualization. **Fengkui Duan:** Writing – review & editing, Supervision, Funding acquisition, Conceptualization. **Shuxiao Wang:** Writing – review & editing, Validation, Resources, Data curation. **Jingkun Jiang:** Writing – review & editing, Resources. **Yafang Cheng:** Validation, Resources. **Hang Su:** Validation, Resources. **Taicheng An:** Writing – review & editing, Resources. **Yongliang Ma:** Validation, Resources. **Takashi Kimoto:** Validation, Data curation. **Tao Huang:** Validation, Data curation. **Kebin He:** Writing – review & editing, Supervision, Funding acquisition, Conceptualization.

Declaration of competing interest

The authors declare that they have no known competing financial interests or personal relationships that could have appeared to influence the work reported in this paper.

Acknowledgments

This work was supported by the National Natural Science Foundation of China (grant number 22188102, 22206098) and the International Science and Technology Innovation Cooperation between the governments of the Ministry of Science and Technology of the People's Republic of China (grant number 2022YFE0105500). Yunzhi Xu thanks the Chinese Scholarship Council for financial support of her study at the Max Planck Institute for Chemistry.

Appendix A. Supplementary data

Supplementary data to this article can be found online at https://doi.org/10.1016/j.envpol.2024.125483.

Data availability

Data will be made available on request.

References

An, Z., Huang, R.-J., Zhang, R., Tie, X., Li, G., Cao, J., Zhou, W., Shi, Z., Han, Y., Gu, Z., Ji, Y., 2019. Severe Haze in Northern China: A Synergy of Anthropogenic Emissions and Atmospheric Processes, vol. 116. Proceedings of the National Academy of Sciences, pp. 8657–8666. https://www.pnas.org/doi/abs/10.1073/pnas.1900125116.

Bian, Y.X., Zhao, C.S., Ma, N., Chen, J., Xu, W.Y., 2014. A study of aerosol liquid water content based on hygroscopicity measurements at high relative humidity in the North China Plain. Atmos. Chem. Phys. 14, 6417–6426. https://acp.copernicus.org/articles/14/6417/2014/.

Boyce, S.D., Hoffmann, M.R., 1984. Kinetics and mechanism of the formation of hydroxymethanesulfonic acid at low pH. J. Phys. Chem. 88, 4740–4746. https://doi.org/10.1021/j150664a059.

Campbell, J.R., Battaglia Jr., M., Dingilian, K., Cesler-Maloney, M., St Clair, J.M., Hanisco, T.F., Robinson, E., DeCarlo, P., Simpson, W., Nenes, A., Weber, R.J., Mao, J., 2022. Source and chemistry of hydroxymethanesulfonate (HMS) in fairbanks, Alaska. Environ. Sci. Technol. 56, 7657–7667. https://doi.org/10.1021/acs.est.2c00410.

Chen, C., Zhang, Z., Wei, L., Qiu, Y., Xu, W., Song, S., Sun, J., Li, Z., Chen, Y., Ma, N., Xu, W., Pan, X., Fu, P., Sun, Y., 2022. The importance of hydroxymethanesulfonate (HMS) in winter haze episodes in North China Plain. Environ. Res. 211, 113093. https://doi.org/10.1021/es00004a024.

Chen, X., Walker, J.T., Geron, C., 2017. Chromatography related performance of the Monitor for AeRosols and GAses in ambient air (MARGA): laboratory and field-based evaluation. Atmos. Meas. Tech. 10, 3893–3908. https://doi.org/10.5194/amt-10-3893-2017.

Cheng, B., Ma, Y., Li, H., Feng, F., Zhang, Y., Qin, P., 2022. Water-soluble ions and source apportionment of PM2.5 depending on synoptic weather patterns in an urban environment in spring dust season. Sci. Rep. 12, 21953. https://doi.org/10.1038/s41598-022-26615-y.

Chu, B.W., Ma, Q.X., Duan, F.K., Ma, J.Z., Jiang, J.K., He, K.B., He, H., 2020. Atmospheric "haze chemistry": concept and research prospects. Prog. Chem. 32, 1–4. https://doi.org/10.7536/pc191230.

Deister, U., Neeb, R., Helas, G., Warneck, P., 1986. Temperature dependence of the equilibrium $CH_2(OH)_2 + HSO_3^- = CH_2(OH)SO_3^- + H_2O$ in aqueous solution. J. Phys. Chem. 90, 3213–3217. https://doi.org/10.1021/j100405a033.

Ding, J., Zhao, P., Su, J., Dong, Q., Du, X., Zhang, Y., 2019. Aerosol pH and its driving factors in Beijing. Atmos. Chem. Phys. 19, 7939–7954. https://doi.org/10.5194/acp-19-7939-2019.

Dixon, R.W., Aasen, H., 1999. Measurement of hydroxymethanesulfonate in atmospheric aerosols. Atmos. Environ. 33, 2023–2029. https://doi.org/10.1016/S1352-2310(98)00416-6.

Duan, F.K., He, K.B., Ma, Y.L., Yang, F.M., Yu, X.C., Cadle, S.H., Chan, T., Mulawa, P.A., 2006. Concentration and chemical characteristics of $PM_{2.5}$ in Beijing, China: 2001–2002. Sci. Total Environ. 355, 264–275. https://doi.org/10.1016/j.scitotenv.2005.03.001.

Eatough, D.J., Hansen, L.D., 1984. Bis-hydroxymethyl sulfone: a major aerosol product of atmospheric reactions of SO_2(g). Sci. Total Environ. 36, 319–328. https://doi.org/10.1016/0048-9697(84)90283-3.

Fountoukis, C., Nenes, A., 2007. Isorropia II: a computationally efficient thermodynamic equilibrium model for K^+–Ca^{2+}–Mg^{2+}–NH_4^+–Na^+–SO_4^{2-}–NO_3^-–Cl^-–H_2O aerosols. Atmos. Chem. Phys. 7, 4639–4659. https://doi.org/10.5194/acp-7-4639-2007.

Fu, X., Wang, S., Chang, X., Cai, S., Xing, J., Hao, J., 2016. Modeling analysis of secondary inorganic aerosols over China: pollution characteristics, and meteorological and dust impacts. Sci. Rep. 6, 35992. https://doi.org/10.1038/srep35992.

Geng, G., Zheng, Y., Zhang, Q., Xue, T., Zhao, H., Tong, D., Zheng, B., Li, M., Liu, F., Hong, C., He, K., Davis, S.J., 2021. Drivers of $PM_{2.5}$ air pollution deaths in China 2002–2017. Nat. Geosci. 14, 645–650. https://doi.org/10.1038/s41561-021-00792-3.

Gilardoni, S., Massoli, P., Paglione, M., Giulianelli, L., Carbone, C., Rinaldi, M., Decesari, S., Sandrini, S., Costabile, F., Gobbi, G.P., Pietrogrande, M.C., Visentin, M., Scotto, F., Fuzzi, S., Facchini, M.C., 2016. Direct observation of aqueous secondary organic aerosol from biomass-burning emissions. Proc. Natl. Acad. Sci. U.S.A. 113, 10013–10018. https://doi.org/10.1073/pnas.1602212113.

Guo, H., Sullivan, A.P., Campuzano-Jost, P., Schroder, J.C., Lopez-Hilfiker, F.D., Dibb, J. E., Jimenez, J.L., Thornton, J.A., Brown, S.S., Nenes, A., Weber, R.J., 2016. Fine particle pH and the partitioning of nitric acid during winter in the northeastern United States. J. Geophys. Res. Atmos. 121 (10), 355. https://doi.org/10.1002/2016JD025311, 10,376.

Huang, L., Zhao, Y., Li, H., Chen, Z., 2015. Kinetics of heterogeneous reaction of sulfur dioxide on authentic mineral dust: effects of relative humidity and hydrogen peroxide. Environ. Sci. Technol. 49, 10797–10805. https://doi.org/10.1021/acs.est.5b03930.

Kok, J.F., Storelvmo, T., Karydis, V.A., Adebiyi, A.A., Mahowald, N.M., Evan, A.T., He, C., Leung, D.M., 2023. Mineral dust aerosol impacts on global climate and climate change. Nat. Rev. Earth Environ. 4, 71–86. https://doi.org/10.1038/s43017-022-00379-5.

Li, G., Lu, D., Yang, X., Zhang, H., Guo, Y., Qu, G., Wang, P., Chen, L., Ruan, T., Hou, X., Jin, X., Zhang, R., Tan, Q., Zhai, S., Ma, Y., Yang, R., Fu, J., Shi, J., Liu, G., Wang, Q., Liang, Y., Zhang, Q., Liu, Q., Jiang, G., 2021a. Resurgence of sandstorms complicates China's air pollution situation. Environ. Sci. Technol. 55, 11467–11469. https://doi.org/10.1021/acs.est.1c03724.

Li, H., Duan, F.K., Ma, Y.L., He, K.B., Zhu, L.D., Ma, T., Ye, S.Q., Yang, S., Huang, T., Kimoto, T., 2018. Case study of spring haze in Beijing: Characteristics, formation processes, secondary transition, and regional transportation. Environ. Pollut. 242, 544–554. https://doi.org/10.1016/j.envpol.2018.07.001.

Li, H., Ma, Y., Duan, F., Zhu, L., Ma, T., Yang, S., Xu, Y., Li, F., Huang, T., Kimoto, T., Zhang, Q., Tong, D., Wu, N., Hu, Y., Huo, M., Zhang, Q., Ge, X., Gong, W., He, K., 2021b. Stronger secondary pollution processes despite decrease in gaseous precursors: a comparative analysis of summer 2020 and 2019 in Beijing. Environ. Pollut. 279, 116923. https://doi.org/10.1016/j.envpol.2021.116923.

Li, J., Carlson, B.E., Yung, Y.L., Lv, D., Hansen, J., Penner, J.E., Liao, H., Ramaswamy, V., Kahn, R.A., Zhang, P., Dubovik, O., Ding, A., Lacis, A.A., Zhang, L., Dong, Y., 2022. Scattering and absorbing aerosols in the climate system. Nat. Rev. Earth Environ. https://doi.org/10.1038/s43017-022-00296-7.

Liu, J., Gunsch, M.J., Moffett, C.E., Xu, L., El Asmar, R., Zhang, Q., Watson, T.B., Allen, H.M., Crounse, J.D., St Clair, J., Kim, M., Wennberg, P.O., Weber, R.J., Sheesley, R.J., Pratt, K.A., 2021. Hydroxymethanesulfonate (HMS) formation during summertime fog in an arctic oil field. Environ. Sci. Technol. Lett. 8, 511–518. https://doi.org/10.1021/acs.estlett.1c00357.

Liu, T., Duan, F., Ma, Y., Ma, T., Zhang, Q., Xu, Y., Li, F., Huang, T., Kimoto, T., Zhang, Q., He, K., 2023. Classification and sources of extremely severe sandstorms mixed with haze pollution in Beijing. Environ. Pollut. 322, 121154. https://doi.org/10.1016/j.envpol.2023.121154.

Ma, T., Furutani, H., Duan, F., Kimoto, T., Jiang, J., Zhang, Q., Xu, X., Wang, Y., Gao, J., Geng, G., Li, M., Song, S., Ma, Y., Che, F., Wang, J., Zhu, L., Huang, T., Toyoda, M., He, K., 2020. Contribution of hydroxymethanesulfonate (HMS) to severe winter haze in the North China Plain. Atmos. Chem. Phys. 20, 5887–5897. https://doi.org/10.5194/acp-20-5887-2020.

Moch, J.M., Dovrou, E., Mickley, L.J., Keutsch, F.N., Cheng, Y., Jacob, D.J., Jiang, J., Li, M., Munger, J.W., Qiao, X., Zhang, Q., 2018. Contribution of hydroxymethane sulfonate to ambient particulate matter: a potential explanation for high particulate sulfur during severe winter haze in beijing. Geophys. Res. Lett. 45 (11). https://doi.org/10.1029/2018GL079309, 969-11,979.

Munger, J.M., Tiller, C., Hoffmann, M.R., 1986. Identification of hydroxymethanesulfonate in fog water. Science 231, 247–249. https://www.science.org/doi/abs/10.1126/science.231.4735.247.

Munger, J.W., Collett, J., Daube, B., Hoffmann, M.R., 1990. Fogwater chemistry at riverside, California. Atmos. Environ. Part B - Urban Atmos. 24, 185–205. https://doi.org/10.1016/0957-1272(90)90025-P.

Nenes, A., Pandis, S.N., Weber, R.J., Russell, A., 2020. Aerosol pH and liquid water content determine when particulate matter is sensitive to ammonia and nitrate availability. Atmos. Chem. Phys. 20, 3249–3258. https://doi.org/10.5194/acp-20-3249-2020.

Olson, T.M., Hoffmann, M.R., 1989. Hydroxyalkylsulfonate formation - its role as a S(IV) reservoir in atmospheric water droplets. Atmos. Environ. 23, 985–997. https://doi.org/10.1016/0004-6981(89)90302-8.

Rao, X., Collett Jr., J.L., 1995. Behavior of S(IV) and formaldehyde in a chemically heterogeneous cloud. Environ. Sci. Technol. 29, 1023–1031. https://doi.org/10.1021/es00004a024.

Reilly, J.E., Rattigan, O.V., Moore, K.F., Judd, C., Eli Sherman, D., Dutkiewicz, V.A., Kreidenweis, S.M., Husain, L., Collett, J.L., 2001. Drop size-dependent S(IV) oxidation in chemically heterogeneous radiation fogs. Atmos. Environ. 35, 5717–5728. https://doi.org/10.1016/S1352-2310(01)00373-9.

Rumsey, I.C., Cowen, K.A., Walker, J.T., Kelly, T.J., Hanft, E.A., Mishoe, K., Rogers, C., Proost, R., Beachley, G.M., Lear, G., Frelink, T., Otjes, R.P., 2014. An assessment of the performance of the Monitor for AeRosols and GAses in ambient air (MARGA): a semi-continuous method for soluble compounds. Atmos. Chem. Phys. 14, 5639–5658. https://doi.org/10.5194/acp-14-5639-2014.

Scheinhardt, S., van Pinxteren, D., Müller, K., Spindler, G., Herrmann, H., 2014. Hydroxymethanesulfonic acid in size-segregated aerosol particles at nine sites in Germany. Atmos. Chem. Phys. 14, 4531–4538. https://doi.org/10.5194/acp-14-4531-2014.

Schuttlefield, J.D., Cox, D., Grassian, V.H., 2007. An investigation of water uptake on clays minerals using ATR-FTIR spectroscopy coupled with quartz crystal microbalance measurements. J. Geophys. Res. Atmos. 112. https://doi.org/10.1029/2007JD00897.

Shaddick, G., Thomas, M.L., Mudu, P., Ruggeri, G., Gumy, S., 2020. Half the world's population are exposed to increasing air pollution. npj Climate and Atmospheric Science 3, 23. https://doi.org/10.1038/s41612-020-0124-2.

Shi, G., Xu, J., Peng, X., Xiao, Z., Chen, K., Tian, Y., Guan, X., Feng, Y., Yu, H., Nenes, A., Russell, A.G., 2017. pH of aerosols in a polluted atmosphere: source contributions to highly acidic aerosol. Environ. Sci. Technol. 51, 4289–4296. https://doi.org/10.1021/acs.est.6b05736.

Song, S., Gao, M., Xu, W., Sun, Y., Worsnop, D.R., Jayne, J.T., Zhang, Y., Zhu, L., Li, M., Zhou, Z., Cheng, C., Lv, Y., Wang, Y., Peng, W., Xu, X., Lin, N., Wang, Y., Wang, S., Munger, J.W., Jacob, D.J., McElroy, M.B., 2019. Possible heterogeneous chemistry of hydroxymethanesulfonate (HMS) in northern China winter haze. Atmos. Chem. Phys. 19, 1357–1371. https://doi.org/10.5194/acp-19-1357-2019.

Suzuki, Y., Kawakami, M., Akasaka, K., 2001. ^{1}H NMR application for characterizing water-soluble organic compounds in urban atmospheric particles. Environ. Sci. Technol. 35, 2656–2664. https://doi.org/10.1021/es001861a.

Tang, M., Huang, X., Lu, K., Ge, M., Li, Y., Cheng, P., Zhu, T., Ding, A., Zhang, Y., Gligorovski, S., Song, W., Ding, X., Bi, X., Wang, X., 2017. Heterogeneous reactions of mineral dust aerosol: implications for tropospheric oxidation capacity. Atmos. Chem. Phys. 17, 11727–11777. https://doi.org/10.5194/acp-17-11727-2017.

Wang, F., Wang, M., Kong, Y., Zhang, H., Ru, X., Song, H., 2022. Spatial and temporal variations in spring dust concentrations from 2000 to 2020 in China: simulations with WRF-chem. Rem. Sens. 14, 6090. https://doi.org/10.3390/rs14236090.

Wang, H., Ding, J., Xu, J., Wen, J., Han, J., Wang, K., Shi, G., Feng, Y., Ivey, C.E., Wang, Y., Nenes, A., Zhao, Q., Russell, A.G., 2019. Aerosols in an arid environment: the role of aerosol water content, particulate acidity, precursors, and relative humidity on secondary inorganic aerosols. Sci. Total Environ. 646, 564–572. https://doi.org/10.1016/j.scitotenv.2018.07.321.

Wang, H., Li, J., Wu, T., Ma, T., Wei, L., Zhang, H., Yang, X., Munger, J.W., Duan, F., Zhang, Y., Feng, Y., Zhang, Q., Sun, Y., Fu, P., McElroy, M.B., Song, S., 2024. Model simulations and predictions of hydroxymethanesulfonate (HMS) in the beijing-tianjin-hebei region, China: roles of aqueous aerosols and atmospheric acidity. Environ. Sci. Technol. 58, 1589–1600. https://doi.org/10.1021/acs.est.3c07306.

Wei, L., Fu, P., Chen, X., An, N., Yue, S., Ren, H., Zhao, W., Xie, Q., Sun, Y., Zhu, Q.-F., Wang, Z., Feng, Y.-Q., 2020. Quantitative determination of hydroxymethanesulfonate (HMS) using ion chromatography and UHPLC-LTQ-orbitrap mass spectrometry: a missing source of sulfur during haze episodes in beijing. Environ. Sci. Technol. Lett. 7, 701–707. https://doi.org/10.1021/acs.estlett.0c00528.

Whiteaker, J.R., Prather, K.A., 2003. Hydroxymethanesulfonate as a tracer for fog processing of individual aerosol particles. Atmos. Environ. 37, 1033–1043. https://doi.org/10.1016/S1352-2310(02)01029-4.

Winkelman, J.G.M., Voorwinde, O.K., Ottens, M., Beenackers, A., Janssen, L., 2002. Kinetics and chemical equilibrium of the hydration of formaldehyde. Chem. Eng. Sci. 57, 4067–4076. https://doi.org/10.1016/S0009-2509(02)00358-5.

Wu, Z., Wang, Y., Tan, T., Zhu, Y., Li, M., Shang, D., Wang, H., Lu, K., Guo, S., Zeng, L., Zhang, Y., 2018. Aerosol liquid water driven by anthropogenic inorganic salts: implying its key role in haze formation over the North China plain. Environ. Sci. Technol. Lett. 5, 160–166. https://doi.org/10.1021/acs.estlett.8b00021.

Xia, W., Wang, Y., Chen, S., Huang, J., Wang, B., Zhang, G.J., Zhang, Y., Liu, X., Ma, J., Gong, P., Jiang, Y., Wu, M., Xue, J., Wei, L., Zhang, T., 2021. Double trouble of air pollution by anthropogenic dust. Environ. Sci. Technol. https://doi.org/10.1021/acs.est.1c04779.

Xing, L., Fu, T.M., Cao, J.J., Lee, S.C., Wang, G.H., Ho, K.F., Cheng, M.C., You, C.F., Wang, T.J., 2013. Seasonal and spatial variability of the OM/OC mass ratios and high regional correlation between oxalic acid and zinc in Chinese urban organic aerosols. Atmos. Chem. Phys. 13, 4307–4318. https://doi.org/10.5194/acp-13-4307-2013.

Xu, B., Shang, J., Zhu, T., Tang, X., 2011. Heterogeneous reaction of formaldehyde on the surface of γ-Al_2O_3 particles. Atmos. Environ. 45, 3569–3575. https://doi.org/10.1016/j.atmosenv.2011.03.067.

Xu, L., Duan, F., He, K., Ma, Y., Zhu, L., Zheng, Y., Huang, T., Kimoto, T., Ma, T., Li, H., Ye, S., Yang, S., Sun, Z., Xu, B., 2017. Characteristics of the secondary water-soluble ions in a typical autumn haze in Beijing. Environ. Pollut. 227, 296–305. https://doi.org/10.1016/j.envpol.2017.04.076.

Xu, L., Fukushima, S., Sobanska, S., Murata, K., Naganuma, A., Liu, L., Wang, Y., Niu, H., Shi, Z., Kojima, T., Zhang, D., Li, W., 2020. Tracing the evolution of morphology and mixing state of soot particles along with the movement of an Asian dust storm. Atmos. Chem. Phys. 20, 14321–14332. https://doi.org/10.5194/acp-20-14321-2020.

Yang, S., Ma, Y.L., Duan, F.K., He, K.B., Wang, L.T., Wei, Z., Zhu, L.D., Ma, T., Li, H., Ye, S.Q., 2018. Characteristics and formation of typical winter haze in Handan, one of the most polluted cities in China. Sci. Total Environ. 613, 1367–1375. https://doi.org/10.1016/j.scitotenv.2017.08.033.

Yin, Z., Wan, Y., Zhang, Y., Wang, H., 2022. Why super sandstorm 2021 in North China? Natl. Sci. Rev. 9, nawb165. https://doi.org/10.1093/nsr/nwab165.

Yu, T., Xiaole, P., Yujie, J., Yuting, Z., Weijie, Y., Hang, L., Shandong, L., Zifa, W., 2023. East Asia dust storms in spring 2021: transport mechanisms and impacts on China. Atmos. Res. 290, 15.. https://doi.org/10.1016/j.atmosres.2023.106773.

Zhang, H., Xu, Y., Jia, L., 2023. Hydroxymethanesulfonate formation as a significant pathway of transformation of SO_2. Atmos. Environ. 294, 119474. https://doi.org/10.1016/j.atmosenv.2022.119474.

Zhang, Q., Zheng, Y., Tong, D., Shao, M., Wang, S., Zhang, Y., Xu, X., Wang, J., He, H., Liu, W., Ding, Y., Lei, Y., Li, J., Wang, Z., Zhang, X., Wang, Y., Cheng, J., Liu, Y., Shi, Q., Yan, L., Geng, G., Hong, C., Li, M., Liu, F., Zheng, B., Cao, J., Ding, A., Gao, J., Fu, Q., Huo, J., Liu, B., Liu, Z., Yang, F., He, K., Hao, J., 2019. Drivers of Improved $PM_{2.5}$ Air Quality in China from 2013 to 2017, vol. 116. Proceedings of the National Academy of Sciences, pp. 24463–24469. https://www.pnas.org/doi/abs/10.1073/pnas.1907956116.

Zhang, R., Wang, G., Guo, S., Zamora, M.L., Ying, Q., Lin, Y., Wang, W., Hu, M., Wang, Y., 2015. Formation of urban fine particulate matter. Chem. Rev. 115, 3803–3855. https://doi.org/10.1021/acs.chemrev.5b00067.

Zhang, Y., Carmichael, G.R., 1999. The role of mineral aerosol in tropospheric chemistry in East asia—a model study. J. Appl. Meteorol. 38, 353–366. https://doi.org/10.1175/1520-0450(1999)038<0353:TROMAI>2.0.CO, 2.

Zhang, Y., Yang, P., Gao, Y., Leung, R.L., Bell, M.L., 2020. Health and economic impacts of air pollution induced by weather extremes over the continental U.S. Environ. Int. 143, 105921. https://doi.org/10.1016/j.envint.2020.105921.

Zhao, B., Wang, S., Hao, J., 2024. Challenges and perspectives of air pollution control in China. Front. Environ. Sci. Eng. 18, 68. https://doi.org/10.1007/s11783-024-1828-z.

Zheng, B., Tong, D., Li, M., Liu, F., Hong, C., Geng, G., Li, H., Li, X., Peng, L., Qi, J., Yan, L., Zhang, Y., Zhao, H., Zheng, Y., He, K., Zhang, Q., 2018. Trends in China's anthropogenic emissions since 2010 as the consequence of clean air actions. Atmos. Chem. Phys. 18, 14095–14111. https://doi.org/10.5194/acp-18-14095-2018.

Zheng, G.J., Duan, F.K., Su, H., Ma, Y.L., Cheng, Y., Zheng, B., Zhang, Q., Huang, T., Kimoto, T., Chang, D., Pöschl, U., Cheng, Y.F., He, K.B., 2015. Exploring the severe winter haze in Beijing: the impact of synoptic weather, regional transport and heterogeneous reactions. Atmos. Chem. Phys. 15, 2969–2983. https://doi.org/10.5194/acp-15-2969-2015.

Zuo, P., Huang, Y., Liu, P., Zhang, J., Yang, H., Liu, L., Bi, J., Lu, D., Zhang, Q., Liu, Q., Jiang, G., 2022. Stable iron isotopic signature reveals multiple sources of magnetic particulate matter in the 2021 Beijing sandstorms. Environ. Sci. Technol. Lett. 9, 299–305. https://doi.org/10.1021/acs.estlett.2c00144.